Quantum entanglement in polarization and space

Lee, Peter Sing Kin

CHAPTER 3

Simple method for accurate characterization of birefringent crystals

We present a simple method to determine the cutting angle and thickness of birefringent crystals. Our method is based upon chromatic polarization interferometry and allows for accuracies of typically 0.1° in the cutting angle and 0.5% in the thickness.

P.S.K. Lee, J.B. Pors, M.P. van Exter, and J.P. Woerdman, Appl. Opt. **44**, *866-870 (2005).*

3.1 Introduction

Birefringent crystals play a key role in various optical applications ranging from polarization manipulations in linear optics to frequency conversion in nonlinear optics. As the specification of ready-made crystal slabs is often limited by manufacturing tolerances, accurate inspection after production is usually required. Properties of birefringent materials are generally characterized by applying interferometric [41–44] or ellipsometric techniques [45–47]. All these techniques enable one to determine the axes of orientation or the refractive indices (or both) of the birefringent material, but not its thickness (apart from [47]). We present here a simple method for simultaneous determination of both the precise cutting angle and thickness of a birefringent crystal. Our method uses the refractive indices of the crystal as input, since these indices are already well-known to high precision for most of the relevant crystals [48]. We combine this input with chromatic polarization interferometry to determine precisely the absolute order of the crystal (acting as a waveplate) at several angles of incidence.

3.2 Theory

When considering plane-wave illumination of a uniaxial waveplate, the accumulated phase difference $\Delta\phi$ between the ordinary and extraordinary light upon propagation through a birefringent crystal is given by

$$\Delta\phi = d(k_{o,z} - k_{e,z}) \,, \tag{3.1}$$

where d is the crystal thickness and $k_{o,z}$, $k_{e,z}$ are the internal longitudinal wavevector components of the ordinary and extraordinary light in the (z-)direction parallel to the surface normal. In detail, the wavevector components are given by

$$k_{o,z} = k_0\sqrt{n_o^2(\lambda) - \sin^2(\theta)} \tag{3.2}$$

$$k_{e,z} = k_0\sqrt{n_e^2(\lambda,\Theta) - \sin^2(\theta)} \tag{3.3}$$

where $k_0 = 2\pi/\lambda$ is the wavevector of the incoming beam, θ is the angle of incidence and $n_o(\lambda)$ and $n_e(\lambda,\Theta)$ are the refractive indices at the specified wavelength λ and angle Θ, with

$$\frac{1}{n_e(\Theta)} = \sqrt{\frac{\cos^2\Theta}{n_o^2} + \frac{\sin^2\Theta}{n_e^2}} \;. \tag{3.4}$$

Here, $\Theta = \theta_c + \theta'$ is the angle between $\vec{k}_e$ and the crystalline c-axis, θ_c is the cutting angle (= angle between c-axis and surface normal), and θ' is the internal refraction angle. All relevant angles are indicated in Fig. 3.1.

Despite the simplicity of the above equations, the analysis of data obtained from chromatic polarization interferometry requires some thought. Experimentally, we measure the wavelength-dependent optical transmission T of the waveplate when it is positioned between two parallel polarizers. By fitting the measured spectral fringe pattern with the theoretical

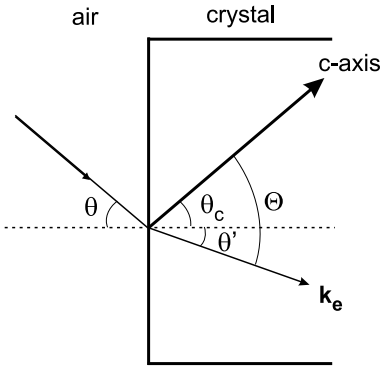

Figure 3.1: *Definition of the relevant angles: angle of incidence θ, internal angle of refraction θ', crystalline cutting angle θ_c, and internal angle Θ.*

expression [49] $T = a\cos^2\{\Delta\phi(\lambda,\theta=0)/2\}+b$, with a and b constant, we can extract not only the fractional but also the *integer* order of the waveplate for any specific wavelength λ_0 (total order is $\Delta\phi(\lambda_0)/2\pi$).

Another issue is the dependence of $\Delta\phi$ on both crystal cutting angle θ_c and thickness d. A single polarization-resolved transmission spectrum contains insufficient information to determine both θ_c and d individually, as a variation of one parameter can be largely compensated for by a change in the other parameter. The basis for this approximate interchangeability of θ_c and d is the observation that Eq. (3.4) is well approximated by its first-order Taylor expansion (as $|n_o - n_e| \ll n_o$), making the refractive index difference $\Delta n(\lambda,\Theta) \equiv n_0(\lambda) - n_e(\lambda,\Theta) \approx \Delta n(\lambda,\Theta=90^\circ)\times\sin^2\Theta$. As a result $\Delta n(\lambda,\theta_c)$ shows a similar wavelength dependence at various cutting angles and differences occur primarily in the prefactor.

To find the individual values of θ_c and d we measure a set of polarization-resolved transmission spectra at various angles of incidence θ. We analyze the spectra obtained at non-normal incidence by using the interchangeability mentioned above: we fit the polarization-resolved transmission spectrum at each incident angle θ by that of a fictitious crystal of effective thickness $d_{\text{eff}}(\theta)$ illuminated at normal incidence, i.e., we write $\Delta\phi(\lambda,\theta)\approx 2\pi d_{\text{eff}}(\theta)\times\Delta n(\lambda,\Theta=\theta_c)/\lambda$. This trick yields a single fitting parameter $d_{\text{eff}}(\theta)$ for every spectrum. As a last step in our analysis we combine the data of all spectra, by plotting $d_{\text{eff}}(\theta)$ (or actually the phase difference $\Delta\phi(\lambda_0,\theta)$ at a fixed wavelength λ_0) versus θ and fitting it with the appropriate expression to extract both the real θ_c and d individually.

With the above trick we avoid the problem that a single spectrum can be fitted with many different (θ_c,d) combinations. The only alternative to our simplified procedure would be a single combined fit of *all* measured spectra. However, such a fit is much more cumbersome.

A nasty detail of every method of analysis is the conversion from external to internal angles; in order to find the internal angle $\Theta=\theta_c+\theta'$ for a given external angle θ and cutting angle θ_c, Snell's law $\sin\theta = n_e(\lambda,\Theta)\sin\theta'$ has to be solved iteratively, since Θ itself depends on θ'. In practice, three iterations are sufficient to find all angles with an error $< 0.0001^\circ$. As a typical example we take $\theta_c = 24.9^\circ$, $\theta = 25^\circ$, $n_o = 1.66736$ and $n_e = 1.55012$; we find then on the first iteration $\theta_1' = \arcsin\{\sin\theta/n_e(\Theta=\theta_c)\} = 14.89^\circ$ and $\Theta_1 = 39.79$, on the second iteration $\theta_2' = \arcsin\{\sin\theta/n_e(\Theta_1)\} = 15.158^\circ$ and $\Theta_2 = 40.058^\circ$, on the third

iteration $\theta_3' = \arcsin\{\sin\theta / n_e(\Theta_2)\} = 15.164^\circ$ and $\Theta_3 = 40.064^\circ$ and the same to within 0.0001° on the fourth iteration. The advantage of our two-step fit procedure is that these iterations are necessary only in the final fit of $\Delta\phi(\lambda_0, \theta)$ versus θ. For the alternative approach of a single complete fit of all data an enormous amount of iterations in the 2-dimensional (λ, θ) space is needed.

3.3 Experimental setup

Figure 3.2 shows the experimental setup. An incandescent lamp (GE 1460X) produces a beam which is directed through two apertures (spaced by 10 cm, each 5 mm diameter) in order to limit its divergence. Note that no lenses have been placed in the beamline. The birefringent BBO crystal (specified cutting angle θ_c = 24.9° ± 0.5° and specified thickness d = 1.0 ± 0.1 mm) is positioned between two parallel polarizers and placed in a rotation stage in such a way that the crystalline optical axis can be rotated in the horizontal plane. A 200 μm diameter optical fiber guides the collected light to a fiber-coupled miniature grating spectrometer (Ocean Optics S2000), which contains a high-sensitivity CCD array for quick and easy measurement of a complete spectrum.

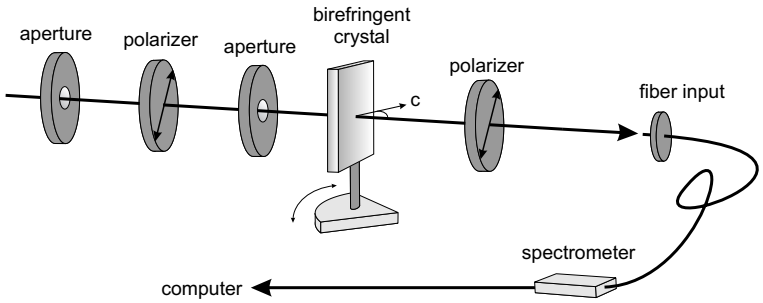

Figure 3.2: *Experimental setup used to measure the optical transmission spectrum of a birefringent crystal sandwiched between two parallel polarizers. Light from an incandescent lamp (not shown) is passed through apertures (to limit its divergence) and the crystal before being spectrally analyzed by a fiber spectrometer. The crystalline c-axis can be rotated in the horizontal plane with an accurate rotation mount.*

In order to generate the phase difference between the ordinary and extraordinary ray, we first orient the crystal's c-axis in the horizontal plane, using both polarizers initially in a horizontal-vertical crossed configuration. The polarizers are then rotated to the 45° setting to get maximum fringe contrast in polarization-resolved transmission.

Since we measure at angles of incidence up to 30°, we paid attention to position the crystal properly along the axis of the rotation stage to avoid (partial) cut off of the light beam by the crystal holder. The scale of the rotation stage is calibrated regarding its zero setting by carefully observing the reflection at normal incidence. Hereby, we could get an accuracy of the zero setting of 0.1°, which is also the accuracy the scale offers for angle measurement.

We operate our spectrometer in the transmission mode, in which the wavelength-dependent light intensity is normalized to the spectrometer signal obtained in the absence of the

crystal. Since this latter signal is relatively weak for wavelengths below roughly 350 nm, the measured signal in the transmission mode is very noisy in this spectral regime. For this reason, we measure in the wavelength domain 400-875 nm, though the fiber spectrometer can operate in the regime 200-875 nm.

3.4 Measurements and results

The experimental part of our method consists of measuring wavelength-dependent transmission spectra $T(\lambda,\theta)$ of the BBO crystal for several angles of incidence θ. Figure 3.3 shows a typical optical transmission spectrum $T(\lambda)$, measured at normal incidence ($\theta = 0$). The modulation depth of the experimentally observed fringes is limited to only $\approx 80\%$ for $\lambda >$800 nm and smoothly decreases to $\approx 30\%$ at $\lambda =$500 nm. We attribute this limitation to the finite opening angle of the light beam, which is approximately 0.7° and mainly determined by the second aperture (5-mm diameter) positioned at 40 cm from the (200 μm diameter) detecting fiber. Multi-beam interference [50] does not play a major role in our experiment since it requires plane-wave illumination, whereas our light source has a finite opening angle and is spatially incoherent.

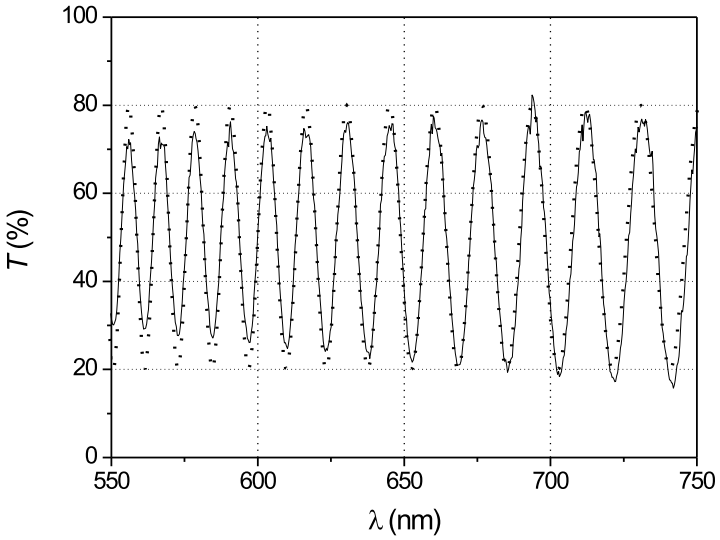

Figure 3.3: *Optical transmission spectrum $T(\lambda)$ of our BBO crystal, which is sandwiched between two parallel polarizers. The measured curve (solid) was taken at normal incidence (θ =0); its best fit (dotted) was found for d_{eff} = 1124 μm and θ_c = 24.7° via the expression $T = a\cos^2[\Delta\phi(\lambda,\Theta=\theta_c)/2]+b$. Note that we present only a part of the full pattern to limit the number of displayed fringes.*

Next, each transmission spectrum is fitted by using the θ=0 expression for the phase

difference, i.e., $\Delta\phi(\lambda,\theta) \approx 2\pi d_{\text{eff}}(\theta)\Delta n(\lambda,\Theta=\theta_c)/\lambda$, with the thickness $d_{\text{eff}}(\theta)$ acting as fitting parameter and θ_c fixed at the *specified* value of 24.9°, which could differ from the real cutting angle. For the spectrum measured at normal incidence, $d_{\text{eff}} = 1124$ μm gives a perfect fit of the fringe period and phase (dotted curve in Fig. 3.3); a precise fit of the fringe amplitudes is not relevant in our analysis. For spectra taken at non-normal incidence (not shown) the fit is not always perfect, simply because the $\theta = 0$ expression is just an approximation, though a good one, for the cases $\theta \neq 0$. To still obtain the correct order $\Delta\phi(\lambda_0,\theta)/2\pi$ at a specific wavelength λ_0, we have to fit with an effective thickness d_{eff} such that experimental curve and fit are exactly in phase at this wavelength (fractional order), while both curves contain an equal number of fringes (= integer order) in the wavelength domain $[\lambda_0, \infty]$. For λ_0 we choose a fixed value of 644 nm, because it is located in the center of our spectral range and accurate refractive index data at this wavelength is available [48]: $n_o = 1.66736$ and $n_e = 1.55012$.

The described fitting procedure works well because we use accurate (at least four decimals) values for the refractive indices n_o and n_e, as tabulated for some wavelengths at T = 293 K in [48] (originally from [51]). Due to the small temperature sensitivity ($\approx 10^{-5}$ K^{-1}) of the refractive indices, temperature fluctuations within 5 K have negligible effect on the refractive index difference, which is of the order of 0.05. The mentioned tabulated values for n_o and n_e served as input to calculate data points for $\Delta n(\lambda,\Theta=\theta_c)$, which are then fitted with the standard dispersion relation (normally used for n) to obtain the full wavelength dependence of $\Delta n(\lambda,\Theta=\theta_c)$ necessary for fitting the observed spectral fringe pattern.

Figure 3.4(a) shows the measured order of waveplate $\Delta\phi(\lambda_0,\theta)/2\pi$ as a function of the incidence angle θ, where each point results from a single spectral measurement. These points are fitted by using the full ($\theta \neq 0$) Eqs. (3.1-3.4) with cutting angle θ_c and thickness d as fitting parameters and λ fixed at $\lambda_0 = 644$ nm, thereby getting the proper internal angle Θ for each θ via iterations. The set of fitting parameters which produces the best fit (solid curve) now gives us the real cutting angle and thickness of our BBO crystal, being $\theta_c = 24.95° \pm 0.1°$ and $d = 1105 \pm 5$ μm. To demonstrate the influence of the fit parameters, we have also plotted two other fits. The dashed curve shows how a change in θ_c (to $\theta_c = 19.95°$, keeping $d = 1105$ μm) leads to something like a horizontal shift of the best fit. The dotted curve shows how an additional change in d leads to a simple and exact scaling in the vertical direction. The new (and incorrect) fit parameters ($\theta_c = 19.95°$, and $d = 1680$ μm) are chosen such that they give the same order of waveplate $\Delta\phi(\lambda_0)/2\pi$ at normal incidence.

To determine the best fit of the data points shown in Fig. 3.4(a), we have calculated the normalized $\chi^2 = \sum_{i=1}^{N} \delta_i^2/(N-2)$ for various sets of fitting parameters θ_c and d (see Table 3.1). Here, N is the number of data points and δ_i are the residuals between data points and fit which, for the best fit, are randomly spread around zero with a standard deviation of 0.10 [see Fig. 3.4(b)]. Besides the real cutting angle θ_c and thickness d of the crystal (minimal χ^2), Table 3.1 also indicates that our method allows for determination accuracies of 0.1° for θ_c and 0.5% for d.

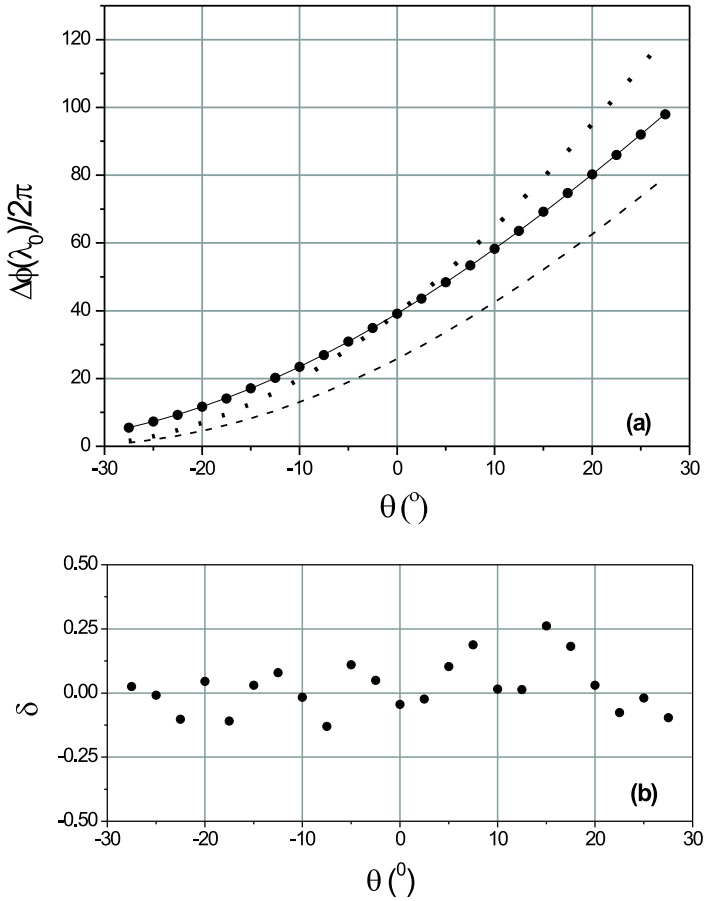

Figure 3.4: *(a) Order of the waveplate $\Delta\phi(\lambda_0,\Theta)/2\pi$ at λ_0 = 644 nm as a function of the angle of incidence θ. The dots are experimental values obtained from fits like the one shown in Fig. 3.3. The solid, dashed and dotted curves are parametric fits (see text for details). (b) Residuals δ between experimental points and best fit shown in (a). The residuals are randomly spread around zero with standard deviation of 0.10.*

3.5 Discussion

As this chapter stresses the high accuracy of our method, we will separately discuss the possible errors in the horizontal and vertical scale of Fig. 3.4(a). The error in the determined angle of incidence θ comes, in the first place, from the scale accuracy of the rotation stage, being 0.1°. In addition, θ can exhibit a systematic error of 0.1° due to the limited accuracy in the calibration of the zero setting of this scale, resulting in a total error in θ of 0.2°. As a consequence of Snell's law, the error in the internal refraction angle is a factor n smaller.

Table 3.1: *Normalized χ^2 as calculated for various cutting angles θ_c and thicknesses* d.

$d(\mu\text{m})$, θ_c	24.85°	24.90°	24.95°	25.00°
1100	0.301	0.170	0.079	0.145
1105	0.106	0.038	0.010	0.022
1110	0.023	0.018	0.054	0.130
1115	0.050	0.109	0.209	0.351

Inaccuracy in the measured order of the waveplate $\Delta\phi(\lambda_0)/2\pi$ comes from improper matching of the experimental curve and fit at λ_0 in the fitting procedure shown in Fig. 3.3. The potential mismatch is, however, not more than a few times 10^{-2} of a fringe, which implies that $\Delta\phi(\lambda_0)/2\pi$ has its error only in the second decimal and can thus be determined more accurately than θ. As we use a simplified fitting procedure (based on d_{eff}), there is a small risk, particularly for large θ, that we miscount $\Delta\phi(\lambda_0)/2\pi$ by a full integer unit due to a miscalculation of the number of fringes in the range $[\lambda_0, \infty]$. Fortunately, such gross errors show up immediately in Fig. 3.4(b) and can thus be easily corrected for.

As an alternative check for the cutting angle, but not for the crystal thickness, we have also used our BBO crystal for type-I second harmonic generation. Starting from a weakly focused laser beam at a wavelength of $\lambda_L = 980$ nm, we found optimum conversion to 490 nm at a measured angle of incidence of $1.2^\circ \pm 0.1^\circ$, corresponding to an internal angle of $\theta' = 0.7^\circ$. With a free software package [52], we determined the angle Θ for optimum conversion [phase-matched by $n_o(\lambda_L) = n_e(\lambda_L/2, \Theta)$]to be $\Theta = 24.3^\circ$. Adding the two values mentioned above leads to a cutting angle $\theta_c = 25.0^\circ$, which agrees well with the value found with our method.

As a test of our method, we have also determined the precise cutting angle and thickness of a second crystal (with specified values $\theta_c = 41.8^\circ \pm 0.5^\circ$ and $d = 200 \pm 20$ μm). Table 3.2 summarizes the results of a series of spectral measurements by giving χ^2 for various θ_c and d. This leads to an actual cutting angle $\theta_c = 41.0 \pm 0.1^\circ$ and thickness $d = 238.5 \pm 0.5$ μm. These small error tolerances are in good agreement with those found with our first crystal, and once more confirm the high accuracy of our method.

We stress that the simplicity of our method is due to the use of well-known refractive indices as input. In solid state optics, characterization of newly developed crystals cannot benefit from this method, as their refractive indices are still unknown, and a much more extensive method is needed. Such a method has been developed by Hecht *et al.* [47], where ellipsometric and polarization transmission intensity measurements are simultaneously analyzed to determine the optical properties of a specific crystal. In addition to its simplicity, our method also allows for easy measurement of any practical crystal thickness, contrary to what is reported in Ref. [47].

Table 3.2: *Normalized χ^2 for a second crystal as calculated for various cutting angles θ_c and thicknesses* d.

$d(\mu\mathrm{m}), \theta_c$	40.85°	40.90°	40.95°	41.00°	41.05°	41.10°
237.5	0.0322	0.0210	0.0124	0.0063	0.0028	0.0019
238.0	0.0183	0.0102	0.0046	0.0016	0.0012	0.0034
238.5	0.0086	0.0036	0.0011	0.0012	0.0039	0.0091
239.0	0.0032	0.0012	0.0018	0.0050	0.0108	0.0192
239.5	0.0019	0.0030	0.0068	0.0131	0.0220	0.0335

3.6 Conclusions

In this chapter, we have presented a simple method, based upon chromatic polarization interferometry, to determine the cutting angle and thickness of birefringent crystals. In spite of its simplicity, the method allows for accuracies of 0.1° in the cutting angle and 0.5% in the thickness, which are generally much smaller values than specified by the manufacturer.

In the present experiment, these accuracies are limited by the quality of the rotation mount. This is, however, not a fundamental limitation. With a more accurate mount, in combination with a better alignment scheme and a less divergent optical beam, even higher accuracies are expected.